Materials Science

http://www.aimspress.com/journal/Materials/

AIMS Materials Science, 8(6): 852–866
DOI: 10.3934/matersci.2021052
Received: 15 September 2021
Accepted: 22 November 2021
Published: 07 December 2021

Research article

Numerical simulations of gradient cooling technique for controlled production of differential microstructure in steel strip or plate

Aarne Pohjonen*

Materials and Mechanical Engineering, Faculty of Technology, University of Oulu, PL4200, 90014 Oulun Yliopisto Oulu, Finland

* **Correspondence:** Email: Aarne.Pohjonen@Oulu.fi; Tel: +358505974261.

Abstract: Numerical studies were conducted to investigate the applicability of cooling strategies for controlledly producing a microstructure in the steel strip or plate, which changes as function of the plate length. In the numerical simulations, the water spray cooling was varied as function of the plate length and as a result, the different parts of the plate were cooled at different rates. We applied the previously developed numerical code where the transformation latent heat is coupled with the heat conduction and transfer model, which has also been calibrated to correspond to experimental laboratory cooling line. The applicability of the method was investigated for controlledly creating alternating bainite and polygonal ferrite regions in plates of two different thicknesses (0.8 cm and 1.2 cm thick plates) by cooling different parts of the plate to different temperatures before switching off the water cooling so that polygonal ferrite forms in the part which has been cooled to higher temperature and bainite forms in the low temperature part. The simulation results indicate that the controlled production of such alternating regions is possible, but the resulting regions in the studied scenario cannot be very thin. The transition regions between the ferrite and bainite regions in the simulated cases are in the range of 5–15 cm. Controlled production of zones consiting of softer phase in the otherwise bainitic steel could offer a possibility for creating designed tracks in a steel bainitic strip or plate, where the mechanical working or cutting of the material is easier.

Keywords: modelling; numerical simulations; differential treatment; temperature control; phase transformations; steel

1. Introduction

Controlled differential treatment of materials offer possibility for tailoring the mechanical properties of the finished or semi-finished part to be suited for a specific application purpose. Differential treatment can include both local mechanical deformation and local temperature control [1, 2]. As

an example, differential heating and cooling has been used in context of hot stamping for producing B-pillars for automobiles, which require high strength at the upper part and lower strength and high plasticity under crash conditions at the lower part. This is achieved by controlling the local temperature of the applied mold [3]. Phase transformations in hot stamping process have been investigated with numerical simulations in [4]. Differential heat treatment has also been used to adjust the mechanical properties of rails by controlling local cooling rate by using controlled mixing of water and air [5]. During differential cooling, distortions can occur since the thermal dilatation and volume changing transformations can occur at different places at different times [6].

In order to control the formation of microstructure during thermomechanical processing, it is very useful to apply numerical simulation methods that are calibrated to correspond to the experimental setting. The virtual experimentation then allows for finding the optimal processing route to meet the needs of a specific application purpose. With the use of the calibrated numerical simulation tools, the thermomechanical treatment of initial material can be optimised to produce the required position dependent mechanical properties in the final product. In the current study, the previously developed and calibrated numerical models for water cooling of steel plate or strip are applied to study the method of producing differential microstructures during cooling by virtual experimentation. In the current context the microstructure was designed to change within centimeter length scale from ferritic to bainitic microstructure. The terms differential treatment and differential microstructure are therefore applied to describe the differences within this length scale in the current study, in the same way as in [1]. The focus of the current study is in application of the numerical modelling to see the feasibility of the approach and the approximate length scales that could be expected for the alternating polygonal ferrite/bainite regions. For the precise control of the regions in applied setting, also experimental trials will be needed to adjust the model parameters to describe the heat transfer corresponding to the cooling devices and the phase transformations occuring in a given steel grade. In the current study the previously developed phase transformation model [7, 8] is fully coupled with heat transfer and coduction model [9–11]. The heat transfer between the water and the steel has been calibrated to correspond to the experimental laboratory water cooling line [12].

The models have been previously used succesfully in the context of simulating phase transformations occuring during cooling of coiled steel strip [13], design of induction hardening of a slurry pipe [14] and for producing ultrafine-structured bainite in a steel plate [15]. In the current article, water cooling is studied as a method for producing the differential cooling rates, but also different cooling methods, such as air cooling [16], mixed air–water [5] or metal contact cooling [17] could be modelled similarly, when the respective heat transfer coefficients are known. Using the numerical model, it was possible to simulate cooling strategies that can be used for creating alternating polygonal ferrite and bainite regions in steel plate or strip.

2. Materials and methods

Current study focuses on the numerical simulations applying the previously published numerical model, described in [9] and [10]. The phase transformation model is based on [7, 18]. The model steel applied in the numerical simulations is described in [10]. The steel composition in wt% was 0.052 C, 0.19 Si, and Mn + Cr = 1.9. In the experiments that were used for the model parameterization (cooling rates from 2 to 90 ^{o}C/s), only ferrite and bainite were observed to form. To provide an overview of

the numerical method, the model is briefly described also here, while the details can be found in the previous publications.

As described in detail in [7, 8], and originally in [19], the transformation onset (assumed to correspond to 1% of austenite transformed to ferritic phase) is calculated with applying the rule of Scheil, i.e. the transformation starts when $\sum_i \frac{\Delta t}{\tau(T)} = 1$, where Δt is the simulation time-step. The function $\tau(T)$ descibed in Eq (2.1) is the time that would be required for the transformation to start during isothermal holding.

$$\tau(T) = K(A - T)^{-m} \exp\left(\frac{Q}{R(T + 273.15)}\right) \tag{2.1}$$

where T is the temperature in °C, A is the limiting temperature for transformation to occur (Ae3 temperature for ferrite and bainite start temperature for bainite), Q is the activation energy for transformation, K and m are fitting parameters. Similar form has been applied already by Kirkaldy [20].

The carbon concentration dependent equilibrium temperature Ae3 defines the condition for ferrite formation above the eutectoid temperature. Ferrite can hold only up to 0.02 wt% carbon. When ferrite forms, the excess carbon is partitioned to the surrounding austenite. When the carbon concentration in the austenite is sufficiently high, so that the local temperature exceeds the Ae3 line, the transformation stops. Below the eutectoid temperature, the maximum ferrite volume fraction is defined by the extrapolated Acm line. These conditions define the temperature dependence of the maximum ferrite fraction that can be transformed from the austenite. The maximum transformed fraction is denoted as $\chi_{\max}$. The carbon concentration dependent equlibrium lines, Ae3 and Acm were calculated using the equations described in [10, 18], but they could also be obtained using thermodynamic softwares.

The transformation kinetics after the onset are calculated applying the Eq (2.2).

$$\frac{d\chi}{dt} = (\chi_{\max} - \chi)\left[\ln\left(\frac{\chi_{\max}}{\chi_{\max} - \chi}\right)\right]^{\frac{n-1}{n}} k^{1/n} \tag{2.2}$$

where $\frac{d\chi}{dt}$ is the transformation rate, χ the previously transformed volume fraction, k the temperature dependent rate parameter and n the Avrami exponent. The maximum fraction takes in to account the remaining austenite, and for the polygonal ferrite the thermodynamical equilibrium fraction for ferrite formation. To model the temperature dependence of the rate parameter, and the effect of carbon on slowing down the bainite formation, we applied the Eq (2.3)

$$\begin{aligned} k_\alpha &= \exp(-a_\alpha(T - b_\alpha)^2 - c_\alpha) \quad \text{for ferrite,} \\ k_b &= \frac{C}{C_\gamma}\exp(-a_b(T - b_b)^2 - c_b) \quad \text{for bainite.} \end{aligned} \tag{2.3}$$

as described in [9, 10]. Formation of the martensite fraction χ_m was simulated using the Koistinen-Marburger Eq (2.4), where the martensite start temperature M_S was calculated using the Stuhlmanns equation [21] and the usual parameter $\eta = 0.011$ was used.

$$\chi_m = [1 - \exp(-\eta(M_S - T))]\chi_{\max} \tag{2.4}$$

The fitted numerical parameters, obtained in the previous study [10] by numerical fitting to continuous cooling experiments, are given in Table 1. These parameters were applied for the phase transformation modelling in the current study.

Table 1. Numerical model parameters.

Product	K	A (°C)	m	Q (kJ)	a	b (°C)	c	n
Ferrite (α)	5.712×10^{-4}	833.8	2.956	184.6	2.079×10^{-4}	775.8	6.359	1.60
Bainite (b)	9.343×10^{-4}	652.7	0.3181	60.0	3.036×10^{-4}	452.2	0.250	2.21

The heat transfer and conduction model, as well as coupling of the latent heat release from the phase transformations was described in detail in our previous publications [9, 10]. Briefly, the 2-dimensional heat Eq (2.5) was solved using explicit finite difference method, which was implemented in Fortran language and parallelized using OpenMP library to enable efficient calculation speed.

$$\rho c \frac{\partial}{\partial t} T = \nabla \cdot (\kappa \nabla T) + s \tag{2.5}$$

where κ is the heat conductivity, t time, and s the latent heat released due to the phase transformations, which is calculated as described in [10, 22, 23]. The determination of the heat transfer coefficient for the laboratory water cooling line is described in [12]. In the rectangular finite difference discretization the plate length (0.564 m) was divided in to 600 segments in the horizontal x-direction. In the vertical y-direction, the plate thickness was divided in to 80 segments for the 1.2 cm and in to 60 segments for the 0.8 cm plate. The simulation timestep was 0.2 ms.

The material is assumed to be initially fully homogenous in the austenitic state in the beginning of the simulation. The initial temperature of the cooled strip/plate is 1000 °C. Two types of differential cooling cases were investigated with numerical simulations described in Sections 2.1 and 2.2. The hypothetical simulated cooling line is defined as having periodic array of water sprays placed regularly apart from each other, with separation distance equal to the plate length Δx. The strip/plate proceeds with a speed of 0.3 m/s at the cooling line. The difference to the actual laboratory water spray cooling line applied in the calibration [12] is that in the real laboratory cooling line, the strip/plate direction is changed periodically (because the short scale of the cooling line), as in the current numerical study the strip/plate propagates continuously in the negative x-direction, corresponding a long line of periodic water sprays.

2.1. Simulation case 1: step interruption in cooling

In the first studied case, the purpose was to see the size of a ferritic region that can be created to the strip/plate by leaving a short segment of the strip/plate at higher temperature, while cooling rest of the strip/plate to the bainitic formation temperature. Figure 1 schematically illustrates the geometry of the strip/plate moving towards left in a cooling line subjected to cooling by periodic array of water sprays, as well as the simulated water cooling strategy for different segments of the plate.

Initially the whole plate is subjected to the water spray cooling with water flux of 6.8 L/m^{2}s. Once the temperature of the plate is in the region where polygonal ferrite forms (~700–780 °C), the step interruption in the cooling is applied, as depicted in Figure 1: the regions A and C are still subjected to water spray cooling, but when the region B is below the water spray, the spray is turned off, so that this region cools only by conduction towards the regions A and C, and by radiation and convection towards the surface directions (up and down in the Figure 1). The formation of ferrite and bainite causes release of latent heat, which is included in the simulation. Once the regions A and C are cooled to the bainitic

formation temperature, no further water cooling is subjected to these regions, so that the whole plate cools by radiation and convection, and internally by conduction within the plate.

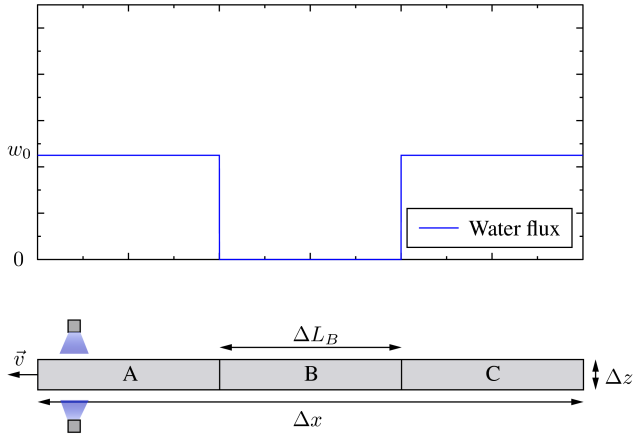

Figure 1. In the simulated case 1, the water cooling was interrupted for the segment B, while segments A and C were subjected to water spray cooling. The strip/plate propagates with velocity $\vec{v}$. The simulations were conducted with altering ΔL_B and Δz. Constant plate length $\Delta x = 56.4$ cm was used in the simulations. The water flux $\omega_0 = 6.8\,\mathrm{L/m^2s}$.

To see how the size of the region B affects the resulting ferrite fraction in this region, simulations were conducted with different lengths of the region, ΔL_B = 2, 4, 6, 8 and 10 cm. To see how the thickness Δz of the strip/plate affects the resulting ferrite fraction, the simulations were conducted with the Δz = 0.8 cm and 1.2 cm thick strip/plate geometries.

2.2. Simulation case 2: gradual change in cooling

In the second investigated case, the purpose was to see how the gradual change in the cooling rate along the lengthwise x-direction of the strip/plate can be utilized to produce smoothly changing microstructure within the plate/strip in this direction. This was realized by changing the simulated water flux gradually from the left side of the plate to the right end of the plate for each water spray in the periodic water spray cooling line, as indicated in Figure 2. The left part (segment A) of the plate is cooled with lower water flux, $\omega_1 = 6.8\,\mathrm{L/m^2s}$. The mid part (segment B) is subjected to linearly rising water flux, and when the right part (segment C) of the plate is under the water spray, higher water flux $\omega_2 = 14.1\,\mathrm{L/m^2s}$ is used to cool this part of the plate. This cooling procedure is repeated every time the plate passes through the water spray zone, so that the segment A is cooled at lower rate and segment C at higher rate and the cooling rate changes gradually within the segment B. The cooling is continued until the right part of the plate is at the bainite formation temperature (~600 °C) and the left part of the plate is at the ferrite formation temperature (~700–780 °C). Once this temperature distribution has been reached, the cooling is stopped so that the whole plate is cooled only by radiation and convection, and internally by conduction within the plate.

To see how the size of the region B affects the resulting ferrite fraction in this region, simulations were conducted with different lengths, ΔL_B = 56.4, 28.2, 14.1, 7.0 and 3.5 cm. To see how the thickness

Δz of the strip/plate affects the resulting ferrite fraction, the simulations were conducted with the Δz = 0.8 cm and 1.2 cm thick strip/plate geometries.

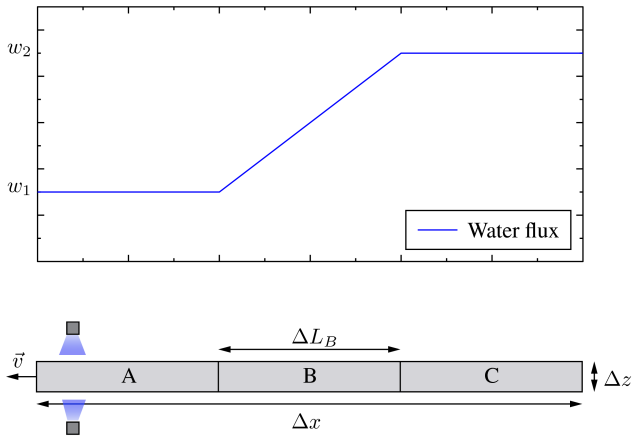

Figure 2. In the simulated case 2, the water flux was linearly changed from lower value w_1 = 6.8 L/m^{2}s to higher value w_2 = 14.1 L/m^{2}s when the segment B is under the water spray. The strip/plate propagates with velocity $\vec{v}$. The simulations were conducted with altering ΔL_B and Δz. Constant plate length Δx = 56.4 cm was used in the simulations.

3. Results and discussion

To illustrate the simulated temperature distribution resulting from the water cooling in the two studied cases, the distribution is shown in Figure 3 for different simulation snapshots for both studied cases. The snapshots show the distribution when the plate passes through the water spray cooling region.

The Figure 3a–c depict case 1 (step interruption) and Figure 3d–f depict case 2 (gradual change). To quantitatively illustrate the temperature changes at different locations, the temperature is plotted along the horizontal x-direction at the upper surface, sub-surface and in the middle of the plate/strip. The Figure 3a–c show the temperature distribution in the snapshots when the plate passes below the water spray. The spray is turned off when region B (desribed in Figure 1) is in the spray cooling zone, which causes temperature to stay higher in this region. The water spray causes sharp drop in temperature on the surface, but a shallow descent in the mid thickness of the strip, in coherence with the previous study [12].

The Figure 3d–f describe the simulation case 2, where the water flux is gradually changing. In the simulated case depicted in the Figure 3d–f, the length of the region B (described in Figure 2), ΔL_B, equals to the whole plate length in this simulation. As the water flux rises when the plate proceeds under the spray, the magnitude of the temperature drop increases. When the temperature drops below the martensite start temperature, the formation of martensite releases latent heat, which slows down the temperature drop at the surface. Also the latent heat released due to polygonal ferrite and bainite transformations are included in the simulations. The results from the two analysed cases are presented in the Sections 3.1 and 3.2.

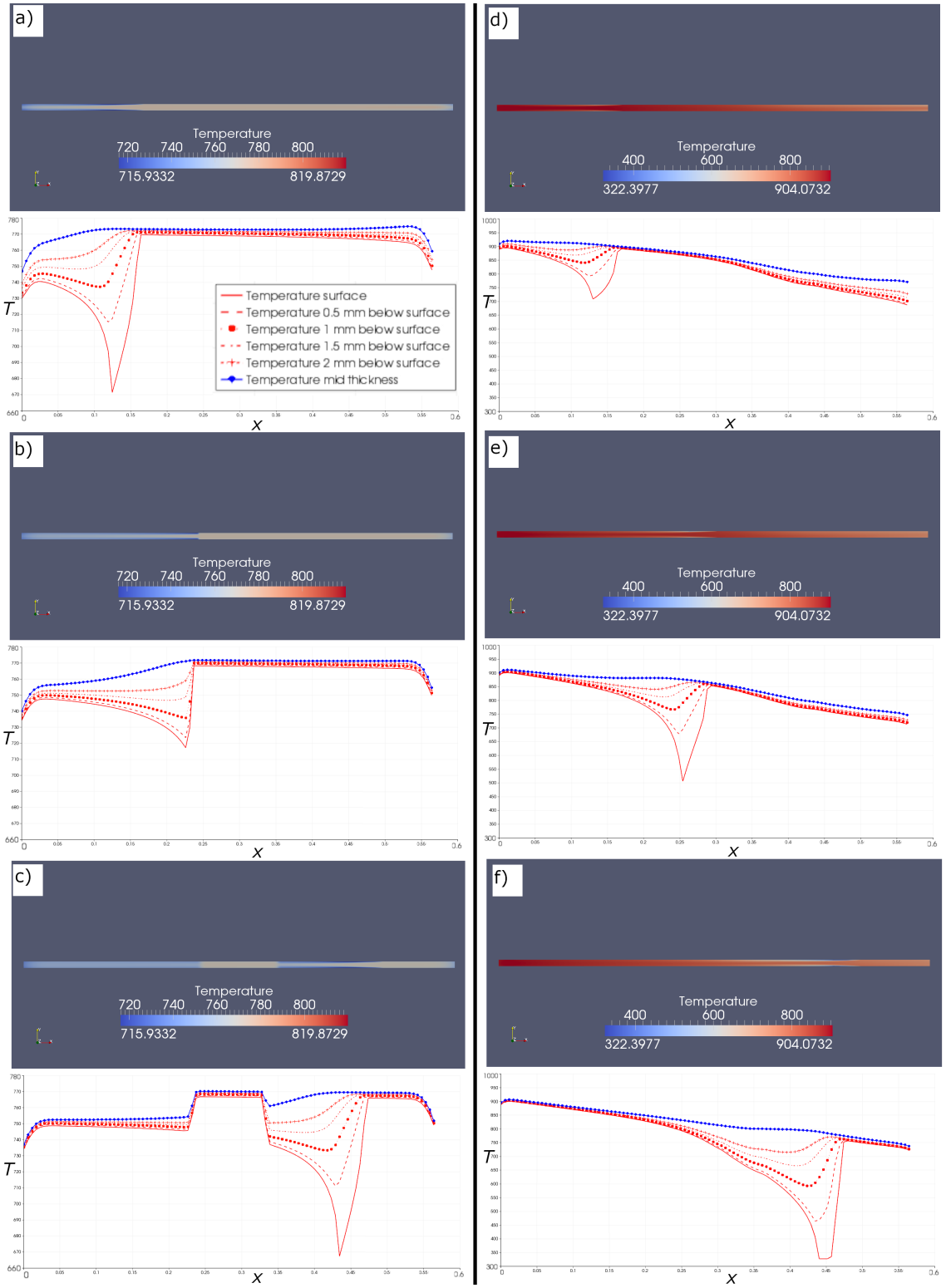

Figure 3. Temperature T (°C) at and near surface (red lines) and in the middle of the plate (blue) along horizontal x direction for simulation snapshots corresponding to the simulated cases (a–c): case 1 (step interruption, ΔL_B = 10 cm, Δz = 0.8 cm), (d–f): case 2 (gradual change, ΔL_B = 56.4 cm, Δz = 0.8 cm). Common legend for all of the figures is shown in (a).

3.1. Simulation case 1: step interruption in cooling

The evolution of temperature and phase fraction distributions along the horizontal x direction in the middle of the plate are shown in Figure 4 for the simulation case study 1. The simulation snapshots are shown for different time instants indicated in the figures. This figure depicts the simulation, where the gap length $\Delta L_B = 10$ cm and plate thickness $\Delta z = 0.8$ cm.

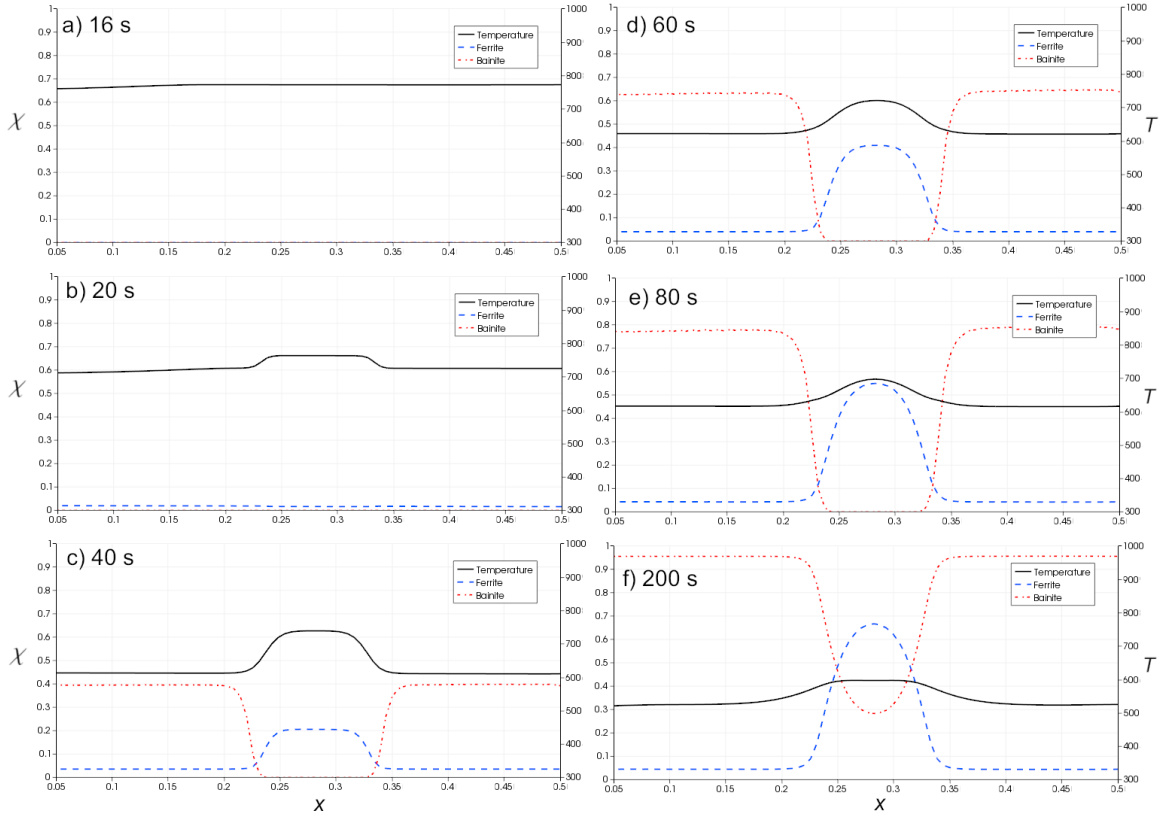

Figure 4. Simulation case 1 (step interruption) with thickness $\Delta z = 0.8$ cm, $\Delta L_B = 10$ cm. χ: transformed fraction, x: x-coordinate (m). T: temperature (°C). Time (s) is indicated in the figures. (a) plate/strip has been uniformly cooled to desired temperature (c–e) ferrite forms at the higher temperature gap region B, bainite forms at the lower temperature regions (A and C) (f) the gap region B contains less bainite.

The result in Figure 4 shows the processes during the simulation: first, (Figure 4a) the whole plate is uniformly cooled to ferrite formation temperateure (~780 °C). (Figure 4b) The spray cooling is continued in the regions A and C (depicted in Figure 1), but not in the region B. The region B is cooled by radiation and convection at the surface boundaries in the vertical y-direction and by conduction towards the regions A and C. The spray cooling of the regions A and C is continued until they are in the temperature range for bainite formation. After this water spray cooling is stopped, and the temperature change within the plate occurs due to radiation, convection and conduction (Figure 4c) Once the temperature in the regions A and C is low enough for the bainite formation (~600 °C), the bainite forms rapidly in comparison to the slowly forming polygonal ferrite. (Figure 4d,e): polygonal ferrite forms slowly in the region B which is at higher temperature. In the transition region between

bainitic and ferritic regions, austenite still stays untransformed for longer time, since this region is in the region where neither ferrite or bainite formation is rapid. (Figure 4f) Once the region B cools to the bainite formation temperature, the remaining austenite transforms to bainite.

The process illustrated in the Figure 4 was similar for the different values of ΔL_B and Δz, but for shorter gap lengths, the cooling occurred faster, resulting to lesser amount of ferrite in the region B, confined in thinner region. Thinner plates also cool faster. The resulting microstructures for different gap lenghts and for two plate thicknesses (Δz = 1.2, 0.8 cm) are shown in the Figures 5 and 6 respectively. Using the simulated cooling strategy, it is possible to produce a softer region consisting of polygonal ferrite within a bainitic steel strip or plate. Controlled production of this kind of regions could offer possibility for producing designed tracks within the plate/strip, where mechanical cutting of the steel is easier.

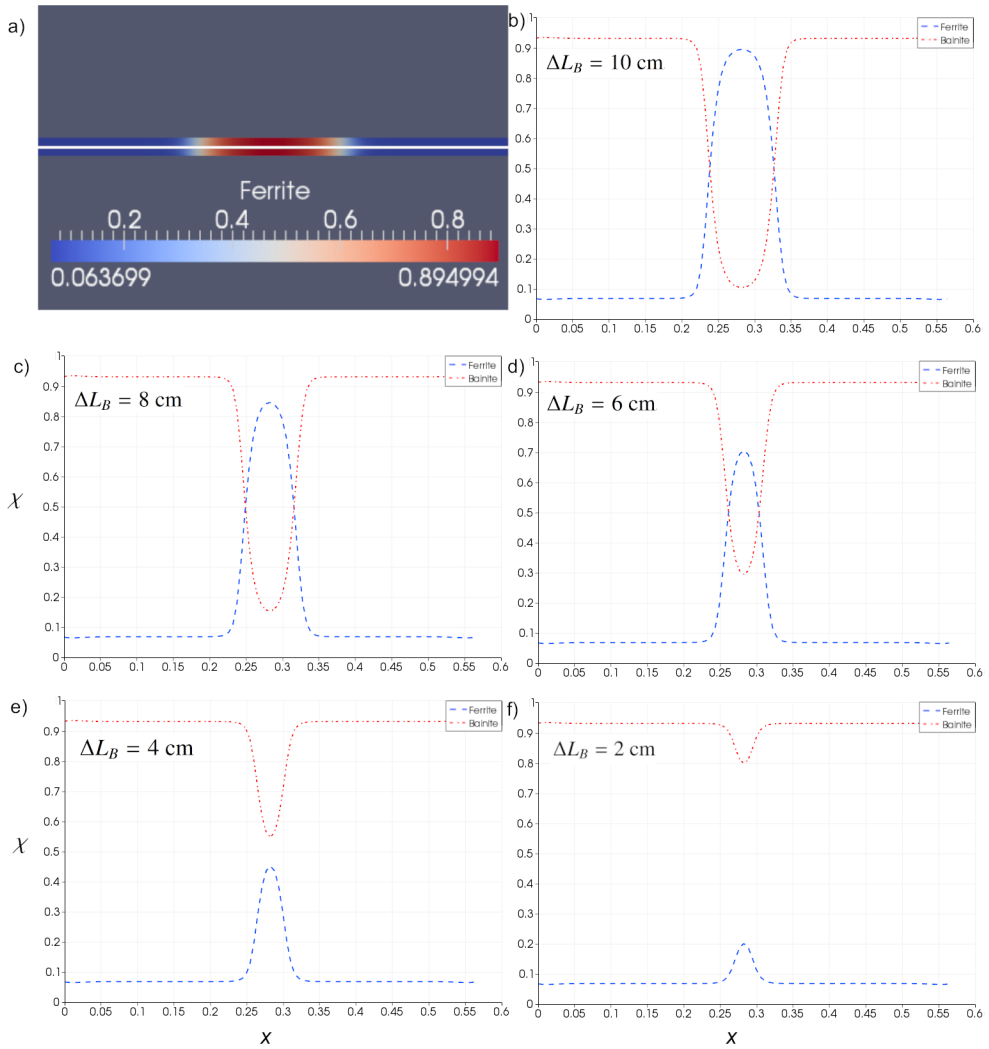

Figure 5. Simulation case 1 (step interruption) with thickness Δz = 1.2 cm, varying ΔL_B. χ: transformed fraction, x: x-coordinate (m). (a) Phase fractions were plotted along the line in the horizontal x-direction, (b) ΔL_B = 10 cm, (c) ΔL_B = 8 cm, (d) ΔL_B = 6 cm, (e) ΔL_B = 4 cm, (f) ΔL_B = 2 cm.

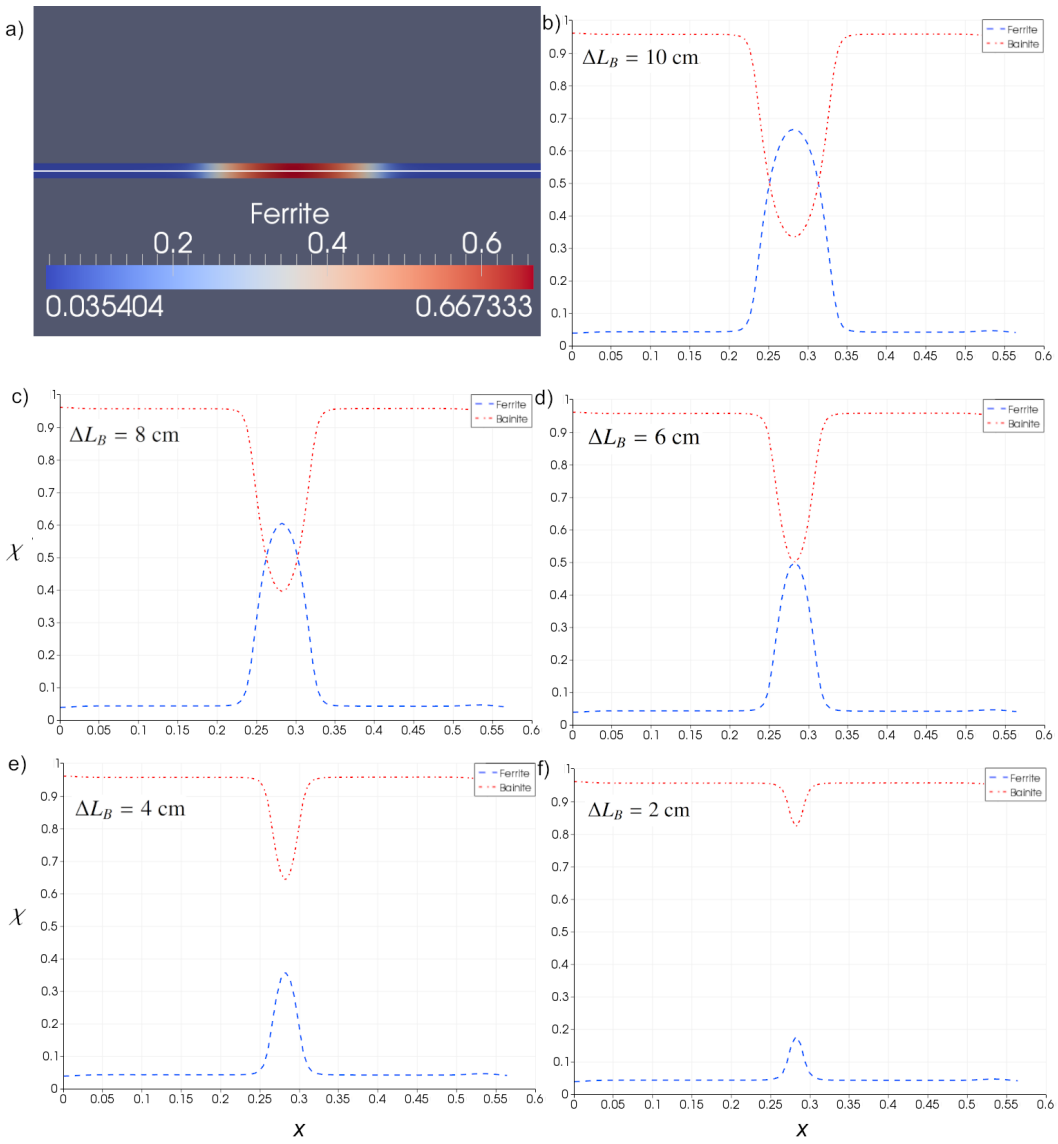

Figure 6. Simulation case 1 (step interruption) with thickness $\Delta z = 0.8$ cm, varying ΔL_B. χ: transformed fraction, x: x-coordinate (m). (a) Phase fractions were plotted along the line in the horizontal x-direction, (b) $\Delta L_B = 10$ cm, (c) $\Delta L_B = 8$ cm, (d) $\Delta L_B = 6$ cm, (e) $\Delta L_B = 4$ cm, (f) $\Delta L_B = 2$ cm.

3.2. Simulation case 2: gradual change in cooling

The evolution of temperature and phase fraction distributions along the horizontal x direction in the middle of the plate are shown in Figure 7 for the simulation case study 2. For the simulation presented in this figure, the length of the transition region (Figure 2) was equal to the whole plate length in the x-direction, i.e. $\Delta L_B = 0.564$ m. (Figure 7a) The right hand side of the plate has been cooled to bainite formation temperature (~600 °C), and large fraction of bainite has formed rapidly. The left hand side is at the ferrite formation temperature range (~700–780 °C), and austenite has started to transform to polygonal ferrite in this region. (Figure 7b,c) The latent heat release due to rapid bainitic

transformation keeps the temperature on the right at almost constant value. On the left, the ferrite forms slowly and the temperature decays slowly due to conduction, radiation and convection. (Figure 7d,e) the left part of the plate is transformed to polygonal ferrie phase and right part is transformed to bainitic phase. At the transition region, large fraction of austenite remains untransformed, since this part is at temperature range between the ferrite and bainite formation temperatures. (Figure 7f) During the slow cooling the remaining austenite is transformed to bainite.

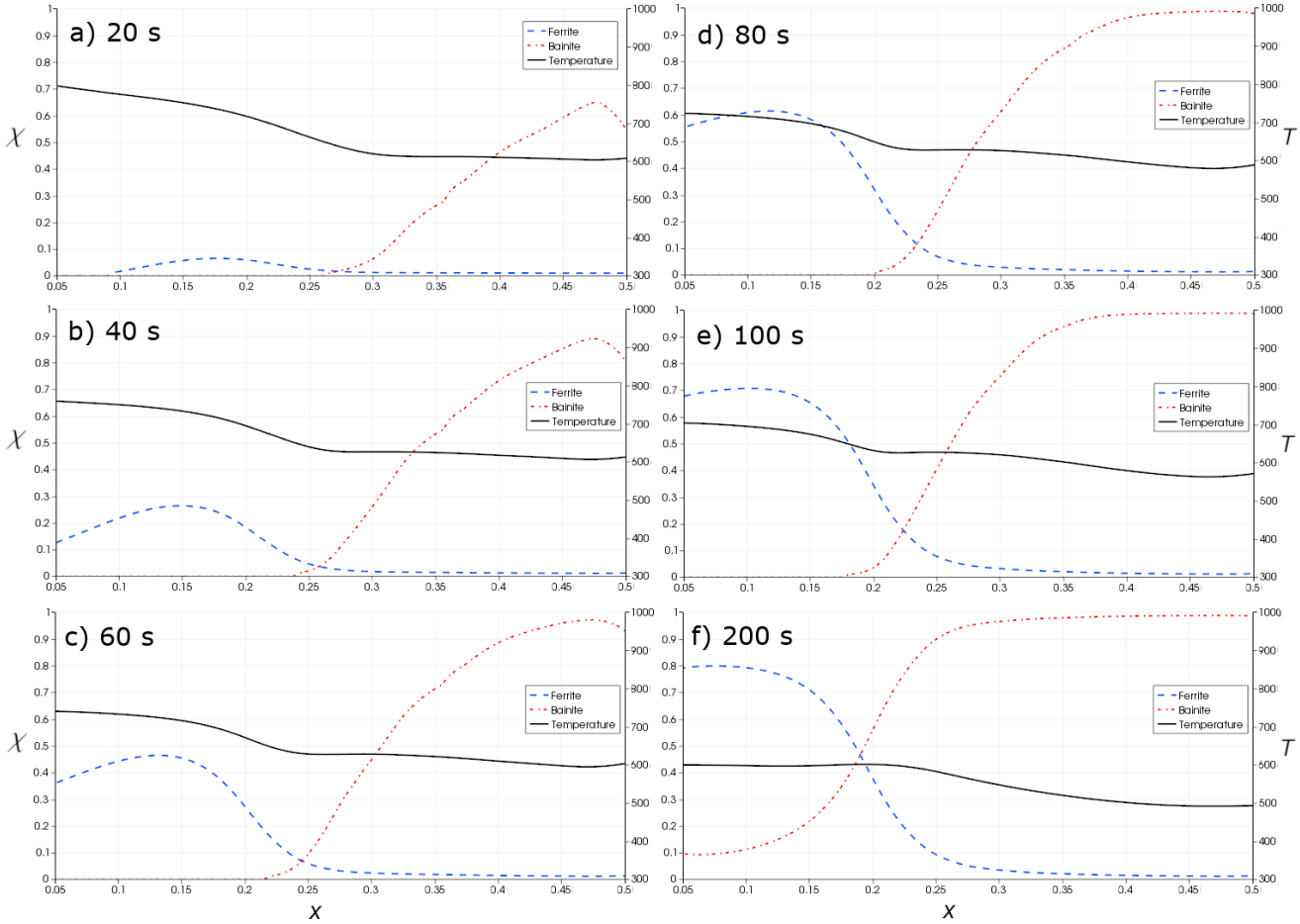

Figure 7. Simulation case 2 (gradual change) with $\Delta L_B = 0.564$ m, $\Delta z = 0.8$ cm. χ: transformed fraction, x: x-coordinate (m), T: temperature (°C). Time (s) is indicated in the figures. (a) bainite has formed on the low temperature region, (b–d) ferrite forms gradually, (e,f) ferrite forms to the final extent and during cooling only small amount of the bainite forms.

The simulations with shorter transition region length, ΔL_B, yielded similar results to Figure 7, but with sharper change in temperature and phase fraction distributions, as expected. The resulting phase fractions obtained from these simulations for two plates of different thickness ($\Delta z = 1.2$ cm, 0.8 cm) and several transition gap lengths ΔL_B are depicted in Figures 8 and 9 respectively. However, when the transition gap length was reduced below 14.1 cm, there was almost no change in the resulting phase distribution.

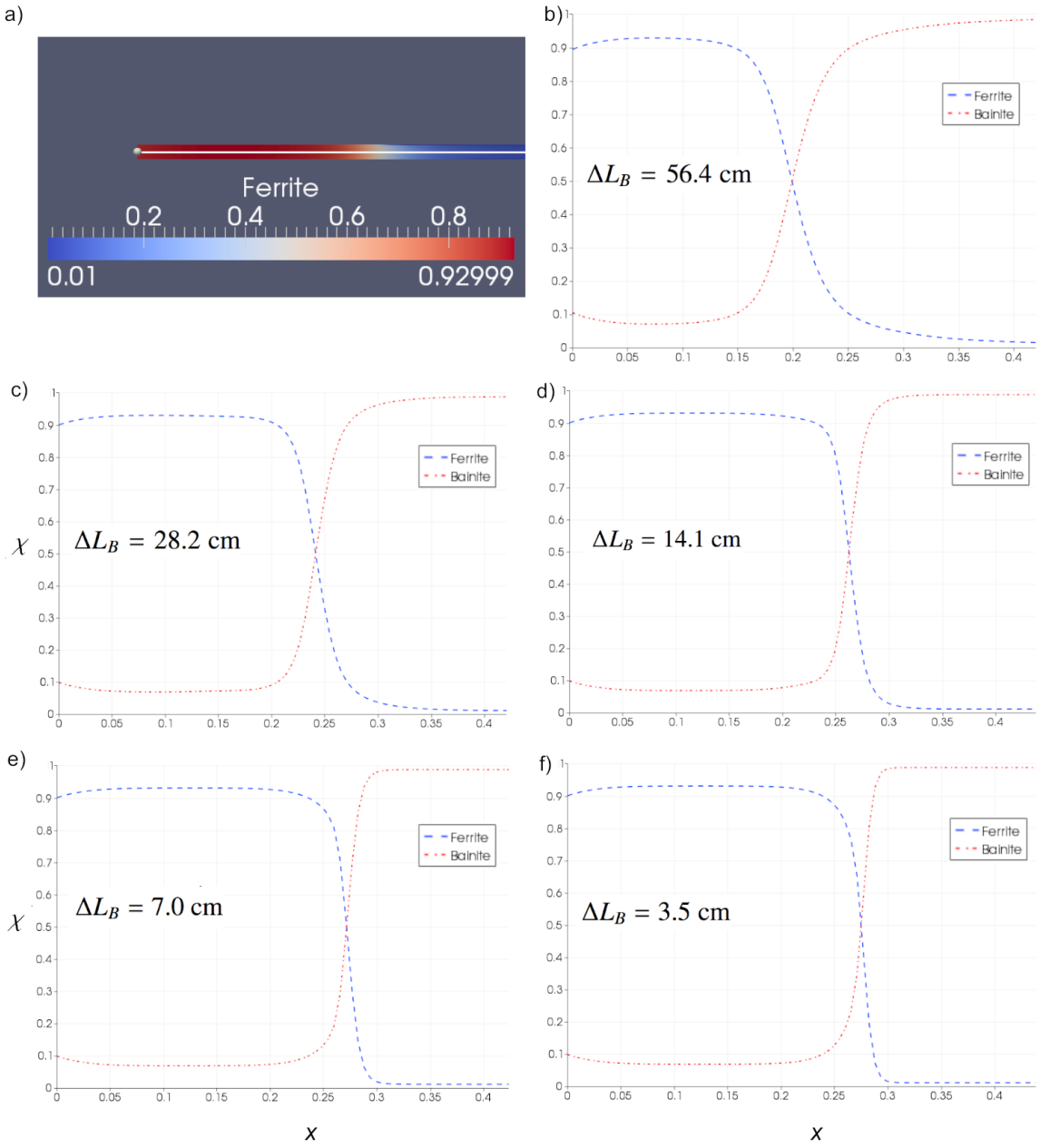

Figure 8. Simulation case 2 (gradual change) with thickness $\Delta z = 1.2$ cm, varying ΔL_B. χ: transformed fraction, x: x-coordinate (m). (a) Phase fractions were plotted along the line in the horizontal x-direction, (b) $\Delta L_B = 56.4$ cm (whole plate length), (c) $\Delta L_B = 28.2$ cm, (d) $\Delta L_B = 14.1$ cm, (e) $\Delta L_B = 7.0$ cm, (f) $\Delta L_B = 3.5$ cm.

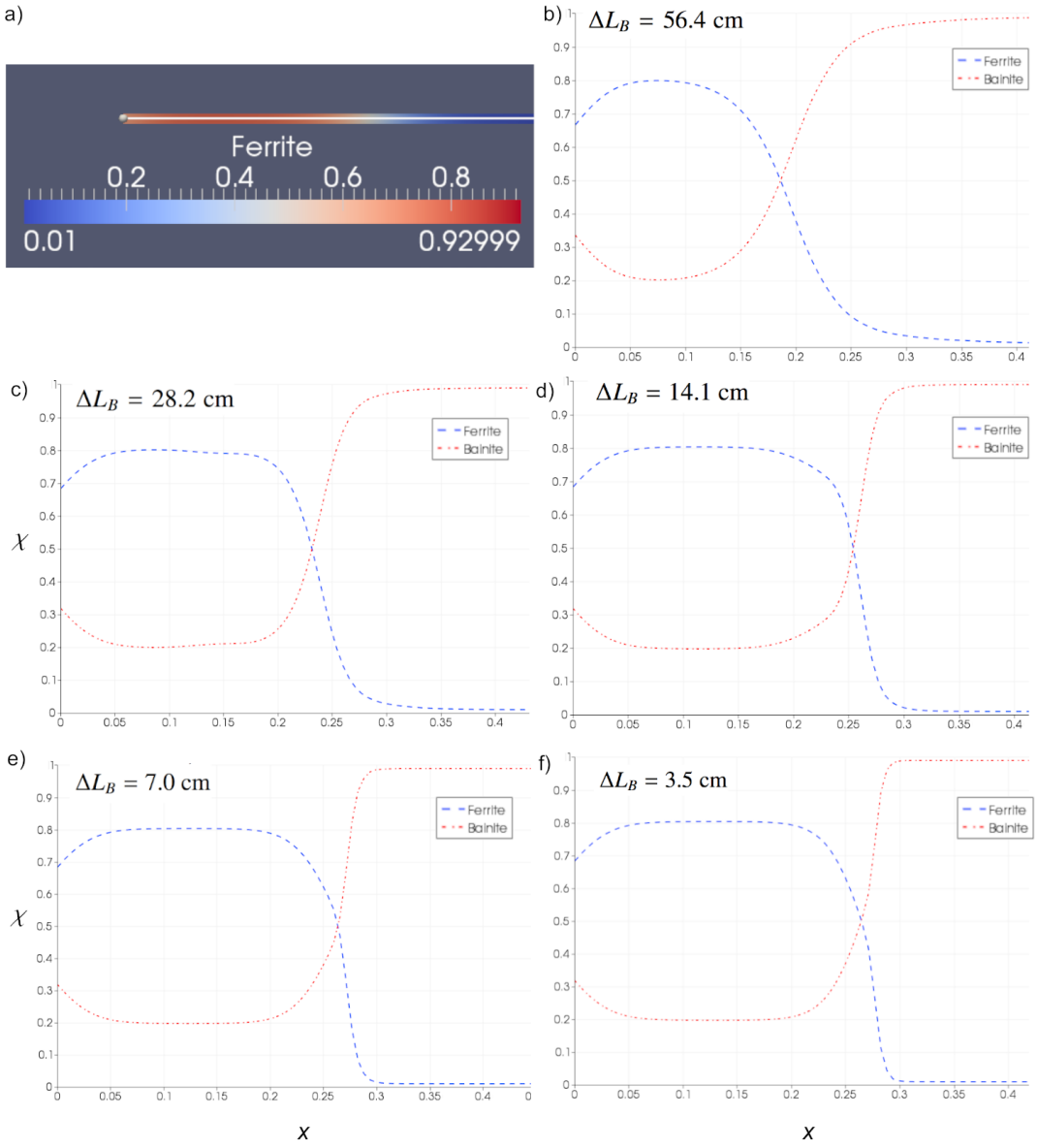

Figure 9. Simulation case 2 (gradual change) with thickness $\Delta z = 0.8$ cm, varying ΔL_B. χ: transformed fraction, x: x-coordinate (m). (a) Phase fractions were plotted along the line in the horizontal x-direction, (b) $\Delta L_B = 56.4$ cm (whole plate length), (c) $\Delta L_B = 28.2$ cm, (d) $\Delta L_B = 14.1$ cm, (e) $\Delta L_B = 7.0$ cm, (f) $\Delta L_B = 3.5$ cm.

4. Conclusions and outlook

Numerical simulations were used for studying controlled production of alternating polygonal ferrite and bainite regions in a steel plate or strip by means of applying differential water spray cooling at different positions of the plate/strip. In the simulations, different regions were cooled to different temperatures, after which the water spray cooling was stopped, so that polygonal ferrite formed in the higher temperature region and bainite formed in lower temperature region. The results show that

differential microstructures can be controlledly created by the differential cooling procedure, but the resulting ferrite/bainite regions in this case should not be expected to be very fine. The simulation results show that transition region between the ferrite and bainite could be controlled to be in the range of 5–15 cm for the applied cooling strategy. Bainite is seen to form rapidly in the low temperature region, and polygonal ferrite more slowly in the high temperature region. In the transition zone between the bainite and ferrite regions, austenite stayed untransformed for longer time. If mechanical forming is applied to the transition region at the time interval when it is still austenitic, it could be easy to form this region in relatively low temperature. The differential cooling strategy could be applied to controlledly create softer ferrite regions in a bainite plate or strip where mechanical cutting would be easier. The polygonal ferrite zones in otherwise bainitic steel could also be applied in a setting where it is desirable to create easily deformable regions at desired positions. In future, the results obtained from the numerical simulations can serve as basis for conducting laboratory scale trials for precise determination of cooling parameters that are needed for accurately producing the alternating ferrite/bainite regions. Future studies could also consider combined heating, cooling, and deformation, as well as extending the simulations for different cooling strategies.

Acknowledgments

The funding of this research activity under the auspices of Genome of Steel (Profi3) project through grant #311934 by the Academy of Finland is gratefully acknowledged.

Conflict of interest

Author declares no conflict of interest.

References

1. Malinov LS (1997) Obtaining a macroscopically nonuniform regular structure in steel by methods of differential treatment. *Met Sci Heat Treat*+ 39: 139–143.
2. Estrin Y, Beygelzimer Y, Kulagin R (2019) Design of architectured materials based on mechanically driven structural and compositional patterning. *Adv Eng Mater* 21: 1900487.
3. Bao L, Nie Q, Wang B, et al. (2019) Development of hot stamping technology for high strength steel parts with tailored properties. *IOP Conference Series: Materials Science and Engineering* 538: 012016.
4. Bok HH, Lee MG, Pavlina EJ, et al. (2011) Comparative study of the prediction of microstructure and mechanical properties for a hot-stamped B-pillar reinforcing part. *Int J Mech Sci* 53: 744–752.
5. Kushnarev AV, Smirnov LA, Kirichkov AA, et al. (2020) Development of an innovative digital cooling technology (differential heat treatment) for Evraz Ntmk rails. *Steel Transl* 50: 415–419.
6. Gale WF, Totemeier TC (2004) Heat treatment, *Smithells Metals Reference Book*, 8 Eds., Oxford: Butterworth-Heinemann, 29-1–29-83.
7. Pohjonen A, Somani M, Porter D (2018) Modelling of austenite transformation along arbitrary cooling paths. *Comp Mater Sci* 150: 244–251.

8. Pohjonen A, Kaijalainen A, Somani M, et al. (2017) Analysis of bainite onset during cooling following prior deformation at different temperatures. *Comput Methods Mater Sci* 17: 30–35.
9. Pohjonen A, Kaijalainen A, Mourujärvi J, et al. (2018) Computer simulations of austenite decomposition of hot formed steels during cooling. *Procedia Manuf* 15: 1864–1871.
10. Pohjonen A, Paananen J, Mourujärvi J, et al. (2018) Computer simulations of austenite decomposition of microalloyed 700 MPa steel during cooling. *AIP Conference Proceedings* 1960: 090010.
11. Ilmola J, Pohjonen A, Seppälä O, et al. (2018) Coupled multiscale and multiphysical analysis of hot steel strip mill and microstructure formation during water cooling. *Procedia Manuf* 15: 65–71.
12. Uusikallio S, Koskenniska S, Ilmola J, et al. (2020) Determination of effective heat transfer coefficient for water spray cooling of steel. *Procedia Manuf* 50: 488–491.
13. Ilmola J, Pohjonen A, Koskenniska S, et al. (2021) Coupled heat transfer and phase transformations of dual-phase steel in coil cooling. *Mater Today Commun* 26: 101973.
14. Javaheri V, Pohjonen A, Asperheim JI, et al. (2019) Physically based modeling, characterization and design of an induction hardening process for a new slurry pipeline steel. *Mater Design* 182: 108047.
15. Pohjonen A, Kaikkonen P, Seppälä O, et al. (2021) Numerical and experimental study on thermomechanical processing of medium-carbon steels at low temperatures for achieving ultrafine-structured bainite. *Materialia* 18: 101150.
16. García Mateo C, Eres-Castellanos A, García Caballero F, et al. (2020) Towards industrial applicability of (medium C) nanostructured bainitic steels (TIANOBAIN). Available from: https://digital.csic.es/handle/10261/217266.
17. Ilmola J, Pohjonen A, Seppälä O, et al. (2020) The effect of internal contact pressure on thermal contact conductance during coil cooling. *Procedia Manuf* 50: 418–424.
18. Donnay B, Herman JC, Leroy V, et al. (1996) Microstructure evolution of C–Mn steels in the hot-deformation process: the stripcam model. *2nd International Conference on Modelling of Metal Rolling Processes*, 23–35.
19. Scheil E (1935) Start time of austenite transformation. *Archiv für das Eisenhüttenwesen* 12: 565–567 (In German). Available from: https://doi.org/10.1002/srin.193500186.
20. Kirkaldy JS (1983) Prediction of microstructure and hardenability in low alloy steels. *Proceedings of the International Conference on Phase Transformation in Ferrous Alloys*, 125–148.
21. Steven W (1956) The temperature of formation of martensite and bainite in low alloy steels, some effects of chemical composition. *J Iron Steel Institute* 183: 349–359.
22. Martin DC (2011) *Selected heat conduction problems in thermomechanical treatment of steel*, Oulu: University of Oulu.
23. Browne KM (1998) Modeling the thermophysical properties of iron and steels. *Proc Mater* 2: 433–438.

AIMS Press